Sudan University of Science and Technology
College of Engineering
Department of Biomedical Engineering

A Project Submitted in Partial Fulfillment for the Degree of B.Sc. in Biomedical Engineering

Monte Carlo simulation of Near-Infrared light-interaction in Diabetic Macular Edema.

Presented by:

Rana Mustafa Awad Al Karim Ismail

Rana Osman Mohammed Osman

Shatha Ezeldin Abdul Rahman Ahmed

Supervised by:

Ola S. Abdalsalam

Oct-2017

بِسْمِ اللَّهِ الرَّحْمَٰنِ الرَّحِيمِ

وَيَسْـَٔلُونَكَ عَنِ الرُّوحِ ۖ قُلِ الرُّوحُ مِنْ أَمْرِ رَبِّي وَمَآ أُوتِيتُم مِّنَ الْعِلْمِ إِلَّا قَلِيلًا ﴿٨٥﴾

صَدَقَ اللَّهُ الْعَظِيمُ

سورة الإسراء الآية 85

Dedication

This thesis is dedicated to

our mothers,

who taught us that even the largest task can be accomplished if it is done one step at a time.

& our fathers,

who taught us that the best kind of knowledge to have is that which is learned for its own sake.

It is also dedicated to

All the kindest people who showered us with their help and support.

Acknowledgement

Abstract

Diabetic Macular Edema (DME) is considered as a major threat to patients that are diagnosed with diabetes. The effects of this disease may lead to severe and even permanent vision lossif timely treatment is not obtained.

This research presented a Monte Carlo simulation - a stochastic type of simulation that is widely used to describe different physical phenomena – of two mathematical models: The normal eye model and the eye that is affectedDiabetic Macular Edema. Each model was divided into a number of layers and each layer is described according to its optical properties. The Monte Carlo simulation software traced the path of individual photons of Near-Infrared light and recorded their interactions with the layers.

This research aims to compare the output of the models to explore and understand the effect of DME on the eye. The important findings of this project is the effect of the disease on the thickness due to the swelling caused by the leak of the fluid from the Blood-Retinal Barrier (BRB) and scattering event which decreased due to the absorption of light by the leaked fluid that are considered the main of the absorbers of the Near-Infrared (NIR) light and the increase of the thickness of the cell bodies that reduce the backscattering light.

We aim to extend the project to simulate the whole retina instead of the three layers that were used and we recommend to continue exploring the other retinal layers effected by DME and also building models for other eye diseases to enrich the information of such cases.

مستخلص

الاستسقاء البقعي يعتبر التهديد الأكبر للمرضى الذين تم تشخيصهم بمرض السكري. تأثير هذا المرض قد يؤدي إلى تأثير حاد وحتى فقدان البصر تماما إذا لم يتم الحصول على العلاج المناسب.

هذا البحث قدم طريقة النمذجة بالمونتي كارلو ــ طريقة إحصائية مستخدمة على نحو واسع لوصف الظواهر الفيزيائية ـ لنوعين من النماذج الرياضية : نموذج العين الطبيعية و نموذج العين المصابة بالاستسقاء البقعي. كل نموذج تم تقسيمه إلى عدد من الطبقات وكل طبقة تم وصفها طبقا لخواصها البصرية. برنامج نمذجة المونتي كارلو تتبع مسار كل فوتون فرديا من ضوء الأشعة تحت الحمراء وسجل تفاعلها مع الطبقات.

هذا البحث يهدف لمقارنة مخرجات النموذجين لاستكشاف وفهم تأثير الإستسقاء البقعي على العين. من أهم النتائج في هذا المشرروع هو تأثير المرض على السماكة نتيجة للإنتفاخ الناتج من تسرب الموائع من الحاجز الدموي الشبكي و حدث الانتثار الذي نقص نتيجة لامتصاص الضوء من الموائع المتسربة التي تعتبر عوامل الامتصاص الرئيسية للأشعة التحت الحمراء القريبة وزيادة سماكة أجسام الخلايا التي قللت من ضوء الأشعة المرتدة.

نحن نهدف إلى توسيع هذا المشوع لمحاكاة طبقة الشبكية كاملة بدلا من الثلاث طبقات المستعملة و نوصي لإكمال اسكتشاف طبقات الشبكية الأخرى المتأثرة بالمرض وأيضا ببناء نموذجات لأنواع أخرى من أمراض العين لإثراء المعلومات لمثل هذه الحالات.

Table of contents

List of Figures

List of Tables

Glossary of Abbreviations

DME	Diabetic Macular Edema
DR	Diabetic Retinopathy
MC	Monte Carlo
MCML	Monte Carlo simulation of Multi-Layered tissues
OCT	Optical Coherence Tomography
ONL	Outer Nuclear Layer
NIR	Near-Infrared
RPE	Retinal Pigments Epithelium

Chapter 1 Introduction

1.1 Background

Diabetic Macular Edema is a consequence of Diabetic Retinopathy that can happen at any level during the disease and it is the leading cause of blindness in diabetic patient [1].The thickening of macula due to the fluid accumulation caused by the breakdown of blood-retinal barrier is the main symptom that defines the disease. The start of the leak happens at the layers of the retina in the back of the eye where many blood vessels carry oxygen and nutrition to nourish the eye. When high sugar levels occur in the vessels it causes occlusion ending by breakdown or creating new blood vessels that may breakdown too due to its weakness. Late treatment of this disease worsens the situation causing blurry vision, black spots in vision and can lead to blindness. Diagnosis of this diseases showing the fundus angiography can be given by fluorescein angiography where the leak can be clearly seen and also the thickening of the macula. Another medical instrument that is very important in diagnosis of eye disease is the OCT (Optical Coherence Tomography). The great advantage this instrument offers such as: non-invasive diagnosis, painless to patient and its high resolution made it a very useful tool. The Near-infrared light (NIR) that the OCT uses, has been used in medical applications for a long time. In this research, NIR light was used to understand the light-tissue interaction in the models of healthy and DME eyes. Mathematical modelling translates what is really happening in the tissue by turning its basic principles into mathematical quantities and expressions (e.g. its optical properties) giving a deep understanding of the phenomenon. To analyze the model, it must be simulated and by simulating, this means imitating or mimicking the behavior of the real-world object or system. One of the best simulation methods that are used is the Monte Carlo simulation. This simulation depends on randomness to give the desired results and that's why it is used in this research to follow the NIR's photons as it interacts with the eye models which consist of multiple layers each one is described by its optical properties.

1.2 Motivation

Due to the prevalence of diabetes; the DR rate in Sudan significantly increased through the years, scoring 82.6% in a recent study [2]. This motivated us to start researching in an attempt to better understand the effect of this disease on the eye components.

1.3 Problem statement

Insufficient information of Near-Infrared light interaction in Diabetic Macular Edema eye.

1.4 Aims and objectives

General

Monte Carlo simulation of Near-Infrared light-interaction in Diabetic Macular Edema.

Specific

1. Exploratory study of the effect of Diabetic Macular Edema (DME) on vision.
2. Comparison between the output signal of the healthy controls and diseased.

1.5 Methodology
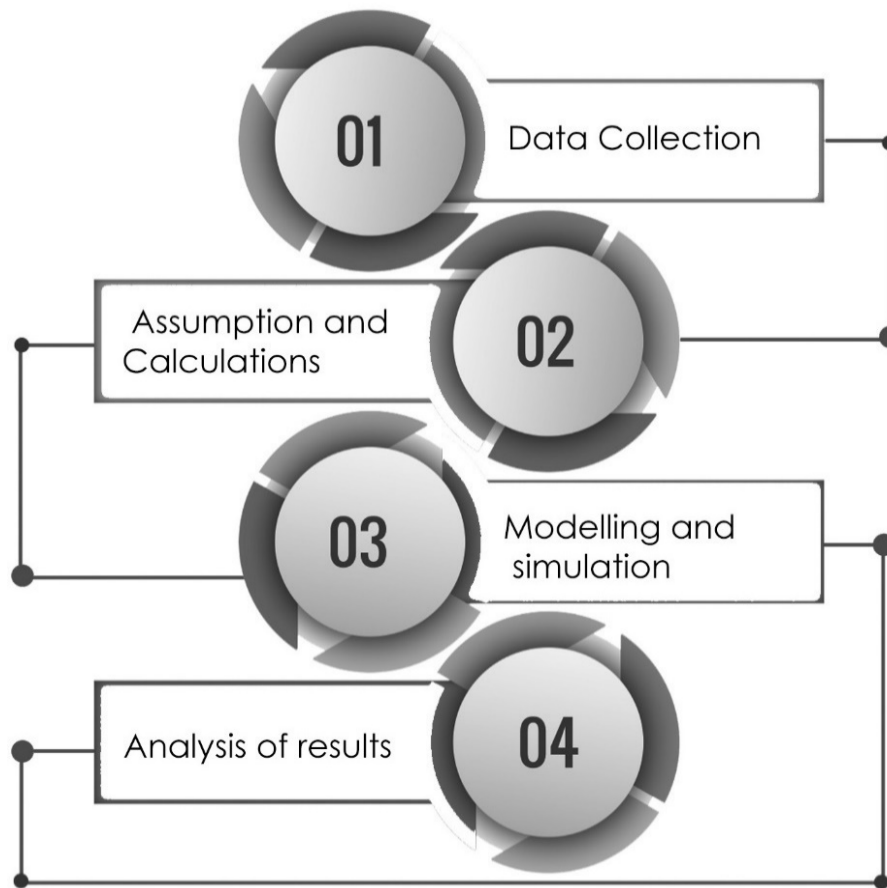
Figure (1.1): Flow chart of the methodology.

1.6 Thesis layout

The thesis for this project consists of: Chapter 1: Provides an introduction and background of the project, and the concerned objectives. Chapter 2: Provides a literature review. Chapter 3: Provides a more detailed theoretical background.Chapter 4: Provides the methodology that has been implemented in the project and the design of the models that has been usedChapter 5:Provides the final results& discussion.Chapter 6: Provides the overall conclusions drawn up from the thesis and some directions that could present as recommendations.

Chapter 2 Literature review

1) **Monte Carlo Simulation of Diabetic Macular Edema Changes on Optical Coherence Tomography Data, Correia, et al (2014)** [3]

Optical coherence tomography (OCT) scans were acquired from healthy controls and patients with diabetic macular edema (DME), a common complication of diabetes characterized by increased retinal thickness due to fluid accumulation. The collected OCT data was divided into three distinct groups: healthy subjects, DME patients with significantly increased outer nuclear layer (ONL) thickness and DME patients without visible changes in the ONL. For each group, the ONL was segmented and processed, yielding a representative A-scan. Using reference values for the physical and optical characteristics of the healthy human retina, a Monte Carlo method with a model for the ONL was used to simulate an A-scan for each group and compare it to the real OCT data. This allowed to identify which alterations in the cellular characteristics are responsible for the changes observed in the OCT scans of the diseased groups. [3]

This paper is the main reason why this thesis was made but the main difference between the two was that the paper studied the eye at a cellular level while this thesis studied it as layers even though the ONL layer used in the paper was the same layer that was focused on in this research. This paper used MCML by (*Lihong et al,1995*)[4] that is also used in this thesis.

2) **Optical Properties of Ocular Tissues in the Near Infrared , Region Yow et al (2007)** [5]

Near infrared characterization of optical properties of various tissue components: Cornea, Vitreous humor, Aqueous humor and lens of healthy human and bovine eyes has been performed. The indices of refraction (n) of these ocular tissues were determined using a Michelson interferometer. The total diffuse reflection (Rd) and total transmission (Tt) measurements have been taken for individual ocular tissue by using double-integrating spheres and infrared laser diodes. The Inverse Adding Doubling computational method based on the diffusion approximation and radiative transport theory is applied to the measured values of *n, Rd,* and Tt to calculate the optical absorption and scattering coefficients of the human and bovine ocular tissues. The scattering anisotropy value was determined by iteratively running the inverse adding doubling method program and a Monte Carlo simulation of light-tissue interaction until the minimum difference in experimental and computed values for Rd and Tt were realized. A comparison between the optical characterization of human and bovine ocular samples is also made. [5]
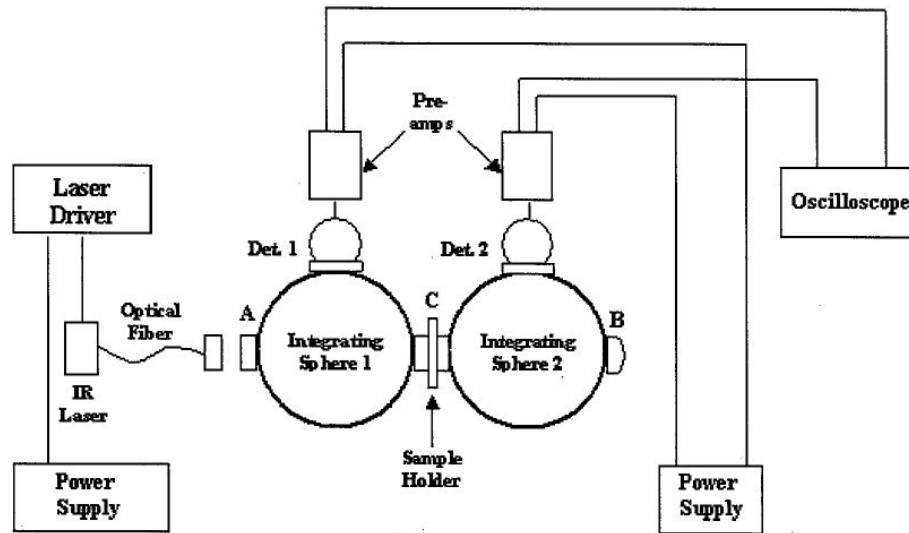
Figure (2.1): Experimental schematic for the measurement of total diffuse reflectance (Rd)and total transmittance (Tt).[5]

This paper is a unique one because it provided many information about the various eye tissue component that has been studied in three wavelengths. The increase and decrease of parameters helped in making convincing assumptions. These parameters can be modeled and used in simulations.

3) The Blood-Retinal Barrier in the Management of Retinal Disease: EURETINA Award Lecture, José Cunha-Vaz (2017) [6]

This paper gives an important and modern overview on the main reason the causes the fluid accumulation on the eyes that are affected with DME.

This group defined the BRB by identifying for the first time the tight junctions that unite retinal endothelial cells and are the basis for the inner BRB, an observation later confirmed in retinal pigment epithelial cells and in brain vessels. A major role of active transport processes was also identified. Today, the BRB is understood to play a fundamental role in retinal function in both health and disease. Retinal edema, a ubiquitous manifestation of retinal disease, is directly associated with breakdown of the BRB and with vision loss. In its most common form (i.e., vasogenic edema), due to breakdown of the BRB, Starling's law of capillary filtration may be used to interpret the mechanisms of fluid accumulation in the retina.[6]

The great information that was provided in this paper helped in better understanding of the disease and how it's been managed such as the main factors involved in the development of retinal edema.Another important thing is that this group introduced an OCT-based method, OCT-Leakage that capable of noninvasively identifying and quantifying sites of alteration of the BRB by

mapping areas of lower-than-normal optical reflectivity, thus reflecting changes in the retinal extracellular fluid

4) Simulation of Cellular Changes on Optical Coherence Tomography of Human Retina, Santos et al (2015). [7]

The paper presented a methodology to assess cell level alterations on the human retina responsible for functional changes observable in the Optical Coherence Tomography data in healthy ageing and in disease conditions, in the absence of structural alterations. The methodology is based in a 3D multilayer Monte Carlo computational model of the human retina. The optical properties of each layer are obtained by solving the Maxwell's equations for 3D domains representative of small regions of those layers, using a Discontinuous Galerkin Finite Element Method (DG-FEM). The DG-FEM Maxwell 3D model and its validation against Mie's theory for spherical scatterers were presented. Also, an application of the methodology to the assessment of cell level alterations responsible for the OCT data in Diabetic Macular Edema was presented. It was possible to identify which alterations are responsible for the changes observed in the OCT scans of the diseased groups. [7]

Chapter 3 Theoretical Background

3.1 Introduction to the human eye

3.1.1 Eye tissue structure
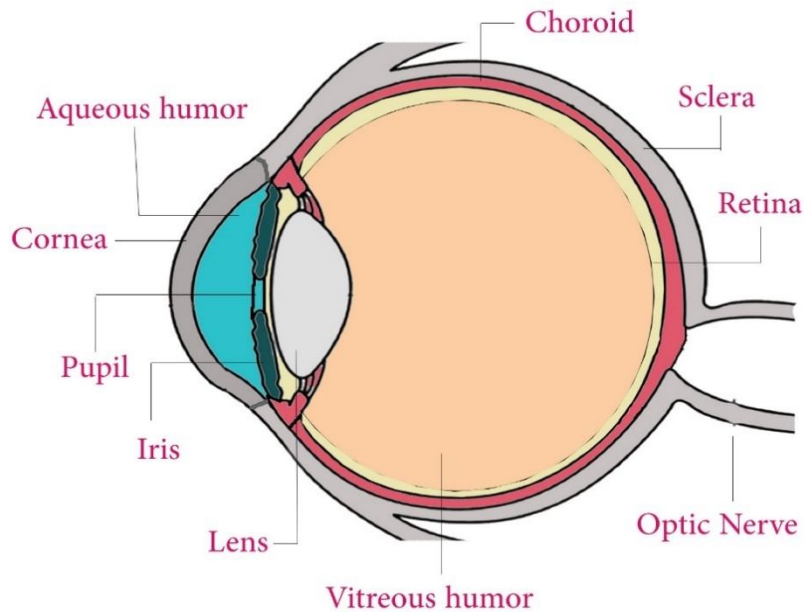
Figure (3.1): Eye tissue structure

As illustrated in the figure above (figure was made by candidates). The human eyeball has three coats, the outer coat sclera, the middle coat choroid and the inner coat retina. The outer coat sclera works as a protective layer where it contains a tough fibrous tissue that preserves the shape of the eyeball and protects the sensitive inner layers. Also, these tough fibrous tissues form the transparent part of the eye, the cornea. The sclera is described as a turbid and a nontransparent medium covering 80% of the eyeball. It mainly comprises conjunctive collagen fibers packed in lamellar bundles submerged within an amorphous ground substance. The corneal stroma is the thickest layer of the sclera and constitutes 90% of the corneal thickness consisting of 50 layers. The middle coat choroid works as a layer of supply where it contains the melanin and rich blood supply. the main structural elements of the middle coat are the pupil, iris & crystalline lens. The pupil represents the circular front that controls the amount and the depth of focus of the entering light on the eye. The iris is a muscular ring that surrounds the

pupil. The lens "commonly known as crystalline lens" even though it has nothing to do with crystal, it leads light rays to the retina, working as a focusing tool. The inner coat retina is a light sensitive layer that works as a receptor for vision that responds to simulation by light and converts that light energy into electric impulses. The retina works at the back of the eye. [8] [9]

3.1.2 Eye tissue study

The cornea

The first layer that the light hits and it's always described as transparent because it's uniform in structure, avascular with a small amount of absorption and with a refractive index that is slightly higher than water. It's approximately spherical and it's composed of several layers. From anterior to posterior [9]:

- Theouter epithelium.
- The basement membrane.
- Anterior limiting lamina (or theBowman's layer).
- Corneal stroma.
- Posterior limiting lamina (or the Descemet'smembrane).
- The epithelium.

Ocular media

Aqueous humor, lens and vitreous humor is always referred as the ocular media. Aqueous humor is the area between lens, cornea and iris. It's often compared to plasma but it contains low amount of proteins and 98% of water but it should not be confused with vitreous humor that holds approximately the same amount of water in a clear gel structure with a viscosity two to four times of water between the lens and retina with no blood vessels[10]. The human lens is almost transparent and with an age-related growth. New fibers are laid over old fibers as it continuously grows and its shape changes too with accommodation and age.

Retinal layers
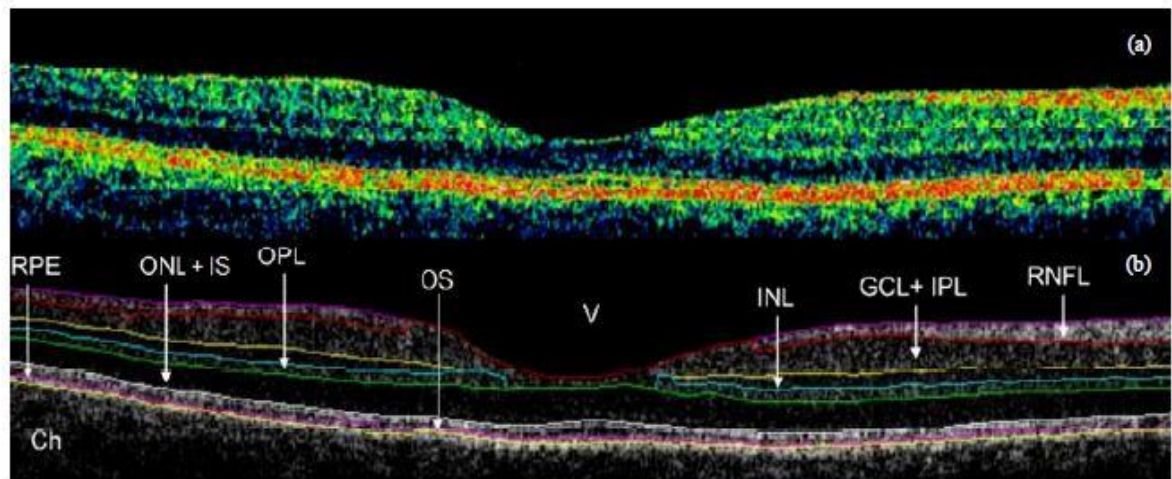
Figure (3.2) : Retinal layers of healthy eyes taken by OCTRIMA [11]

1) *Ch*

   Choroid. The middle coast of the eye and it's located under the last layer of the retina.
2) *GCL*

   The ganglion cell layer.
3) *IPL*

   Inner Plexiform layer
4) *RNFL*

   Retinal Nerve Fiber Layer
5) *INL*

   Inner Nuclear Layer
6) *OPL*

   Outer plexiform layer
7) *ONL*

   Outer Nuclear Layer
8) *IS & OS*

   Inner segment of photoreceptors & outer segment of photoreceptors junction.
9) *RPE*

   Retinal Pigment Epithelial layer

   Sclera

The sclera can be seen as an extension of the cornea with a hole of optic nerve that allows the pass of vessels and nerves.

3.1.3 Outer Nuclear Layer (ONL)

ONL is one of the retinal layers. It comprises the rod and con cell bodies. The rod cell body and nucleus is smaller than those of the cone. The outer fibers of the cone are very short so its nuclei lie in a single layer near the external limiting membrane and inner to the cone cell bodies, several rows of rods cell bodies are arranged.

ONL thickness is 4 rows thick at the temporal edge, 8 to 9 cells thick on the nasal edge and approximately 10 layers thick of cone nuclei in the fovea. [12]

In DME, the fluid accumulation of BRB thickens the macula and the retinal layers. This increase in thickness reduce the backscattered signal compared to normal eyes. [3]

3.2 Diabetic Macular Edema (DME)

Diabetic Macular Edema (DME) is defined nowadays as a disease that threatens diabetes patients with Diabetic Retinopathy (DR) vision acuity.

DME happens when a swelling and thickening in the macula is observed which result in it working improperly that may lead to vision loss.

In diabetes when the pancreas fails to produce sufficient insulin which effects the body's natural ability to maintain a normal level of blood glucose. High blood glucose damages the blood barriers in the eye and this may leak blood or other fluid in it then this leaking fluid can cause the macule to swell, leading to dangerous effects such as vision threatening diseases like DR &DME.[1][6]

3.2.1 Blood-Retinal Barrier (BRB)

DME is depicted by vascular leakage, tissue edema and hard exudates in the center of the retina. To maintain healthy eyes, blood vessels supplies oxygen and nutrition including very small blood vessels that nourishes the retina. When Diabetic Retinopathy worsens, an occlusion in blood vessels may occur which make it a hard job to transport oxygen and nutrition. The eye tries to compensate that loss by creating new blood vessels but unfortunately these blood vessels are weak and are most likely to bleed and accumulate fluid that increases the thickening of the retina causing edema. These factors affect the formation of retinal edema [6]:

1)BRB permeability

An increase in permeability damages the retinal vessel walls.

2) Capillary hydrostatic pressure

An autoregulation by blood flow inhibits capillary hypertension, dilatation, and breakdown of the barrier. Hydrostatic pressure does not affect retinal edema only if it overcame autoregulation.

3) Tissue hydrostatic pressure

Here the tissue becomes weak with low resistance and high compliance that leads to accumulate fluid.

4) Tissue osmotic pressure

If assumed that the amount of proteins in vitreous and retinal extracellular space are the same this allows the proteins to step outside the barrier causing an edema.

3.2.2 Diagnosis of DME

The traditional diagnosis of the disease is the fundus biomicroscopy, fundus stereophotography or both [13]. Fluorescein angiography is also a very useful tool where a special fluorescent dye highlights when it's injected inside the eye then a photo is captured. Fluid accumulation can be seen in the photo but it doesn't give much details as in Optical coherence tomography.

Optical Coherence Tomography

Optical Coherence Tomography (OCT) is a medical diagnosis instrument that is used in a wide range and specially ophthalmology.

It produces a cross-sectional and high-resolution image from 1-15µm. The technique that OCT uses is similar to ultrasound B-mode imaging except that instead of echo sound, OCT uses backscattered light or back-reflected light. [14] [15].

What makes the OCT special, is the following advantages:

- It doesn't used radiation as a source; instead it uses Near-Infrared light.
- Nothing gets injected or digested into the body. So, it's considered a non-invasive method.
- It's not harmful or painful for the patient.
- It doesn't require a lot of time.
- Images can be two-dimensional or three dimensional.
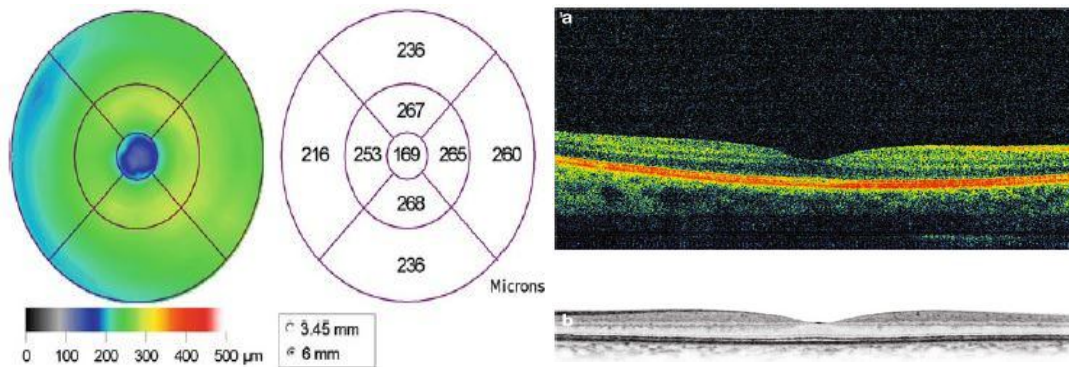
Figure (3.3): Left; two-dimensional color-coded RT map and its numerical representation from a healthy volunteer. Right; SD-OCT, Cirrus: normal cross-sectional macular image; (**a**) false color; (**b**) gray scale [16]

3.3 Optical properties

Optical properties of a tissue describe how it interacts with lightdefining its main characteristics.

Optical properties differ from tissue to another according to its type of light, light interactions, wavelength, energy, intensity of light and its radius.

3.3.1 Light-tissue interactions

When a light beam hit a surface of a matter three types of interactions happens. (The following figures in this section were made by candidates)
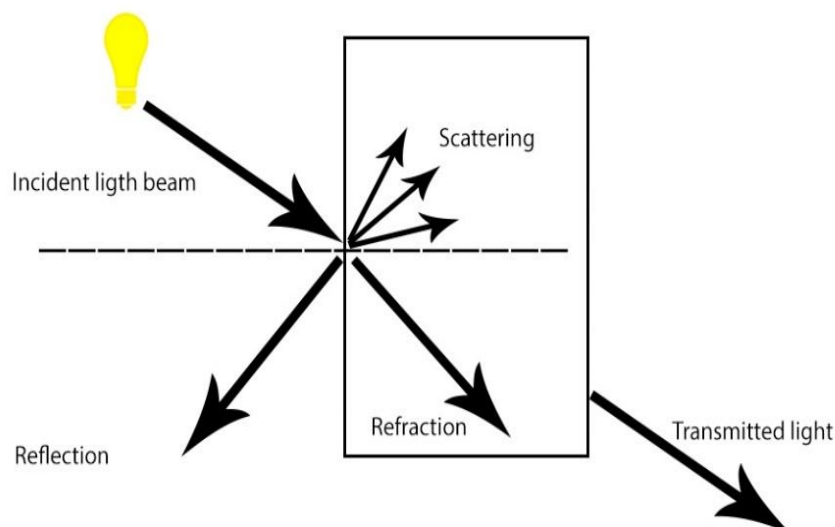
Figure (3.4): Light interactions.

Reflection and Refraction

Reflection is a change of the light beam direction in the interface between two media and returns the light back from where its originated.

Refraction is a change in the speed of the light beam.
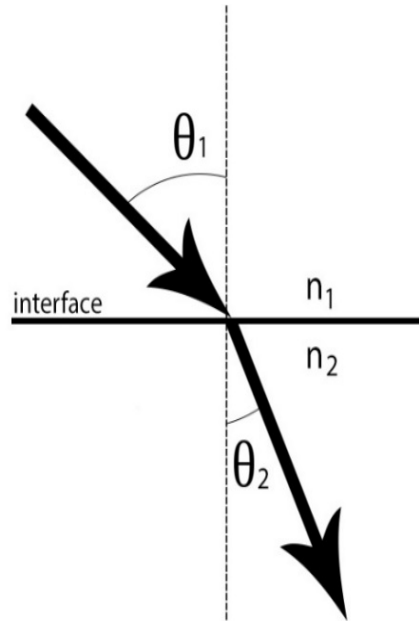
Figure (2.5): Refraction of light. n1=refractive index of incident light media, n2=refractive index of the refracted light media.

The relationship between the reflection and refraction is expressed by the following mathematical equation known by Snell's law:

$$\frac{\sin\theta 1}{\sin\theta 2} = \frac{n2}{n1} \qquad\qquad (1)$$

Absorption

Loss of energy from light by different types of molecules.
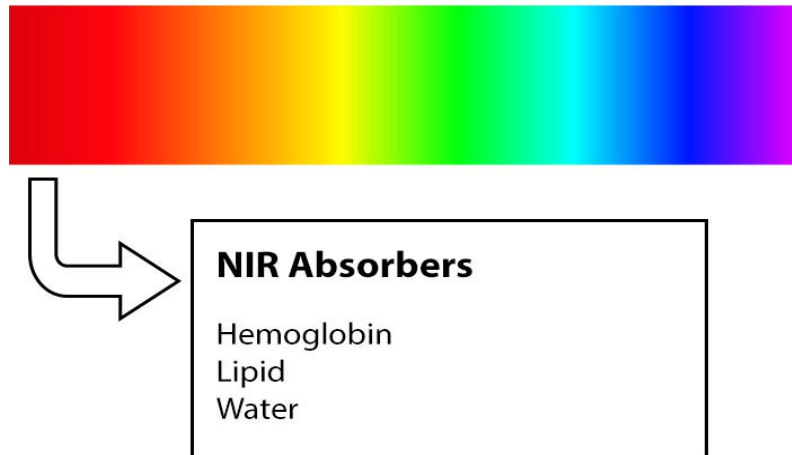
Figure (2.6): Near-Infrared main absorbers

Scattering
Deviation of light from its initial path to other paths.

The light-tissue interaction depends on:

- Structure of tissue
- Optical properties of tissue
- Distribution of light
- Wavelength of light

3.3.2 Other optical properties

- *Physical thickness*
- *Anisotropy factor*
  The average cosines of a scattering angle.
- *Transmission*
  Amount of light that left the tissue after being absorbed and scattered.
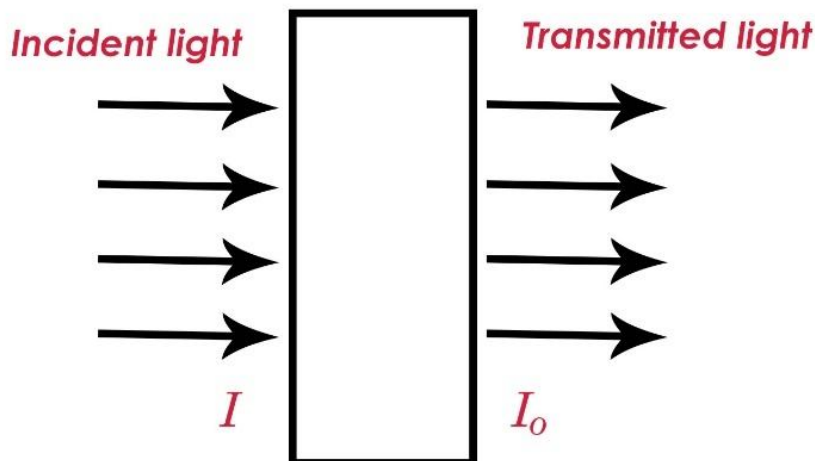
Figure (3.7): Transmission of light

$$T = \frac{I_o}{I} \quad (2)$$

Where I = Intensity of incoming light, I_o = Intensity of outcoming light

- *Optical depth*
  A dimensionless quantity that represents the natural logarithm of transmitted light.
  $$\tau = t(\mu_s + \mu_a) \quad (3)$$

- *Albedo*
  A dimensionless quantity that represents the amount of light reflected without absorption.
  $$a = \mu_s / (\mu_s + \mu_a) \quad (4)$$

3.3.3 Near-infrared light (NIR)

Near-Infrared is a region within the infrared electromagnetic radiation that has a longer wavelength than the visible range. It was first discovered in 1800 by

astronomer Sir William Herschel. Referring it to "radiant heat", Sir William Herschel observed a heating effect when he used a big glass prism to divide the sunlight t onto three thermometers with carbon-blackened bulbs.

Main properties of NIR:

Table (3.1): NIR main properties.[17]

Wavelength	Frequency	Energy	Temperature
0-75-1.4 µm	214-400 THz	886-1653 meV	3591-1797 ℃

3.4 Modelling

Modelling which is usually abbreviated from "Mathematical modelling" is an important subject in mathematics that has been studied over the years. Modelling can be defined as a simplified example of a complex phenomenon depicted by mathematical expressions. Models differ according to a set of principles that governs it, that's why creating a model requires mathematics besides the specialized science field of the phenomenon. Another skill that is highly demanded while creating a model, is the ability to make convincing assumptions and guesses because gathering and acquisition of information about a certain model and its properties might not be as easy as it looks; some information may not be available.

3.4.1 Phases of mathematical modelling
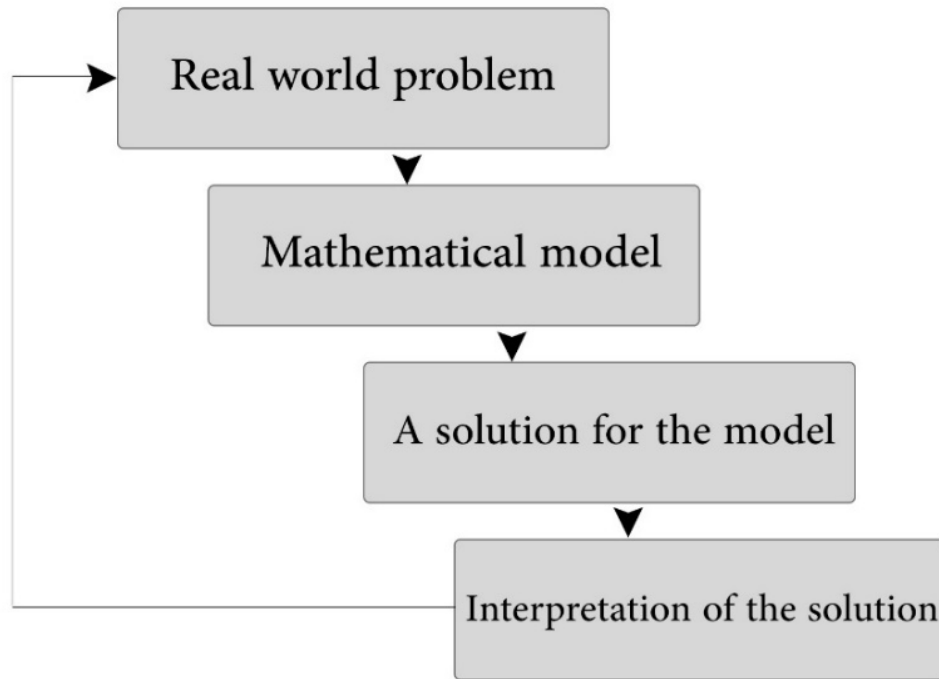
Figure (3.8): Phases of mathematical modelling [18]

First of all, a clear identification of a real problem that need to be solved must exist. Then, as it was explained earlier in the definition of modelling it was clear that it is based conceptual level. So, the core of the construction is all about the mathematical terms, variables and structure of the object that needs to be modeled. It also includes additional efforts like assumptions and simplification. Now, the model is ready to be used in solving the problem that its created for. The development that happened through the years since the evolution of electronics and electrical devices made solving problems easy by the aid of a computer. Most of the models nowadays are being tested by a computer and barely there is no manufacturing company that does not use it. This kind of tests is called simulation. In simulation, you can get the bigger picture of the model's behavior. One of the most widely used simulations, Monte Carlo method will be discussed later. However, the last phase is about justifying and comparing the outcomes. It can also be the end of understanding a problem or a beginning that arises new questions.

3.5 Monte Carlo Simulation

Monte Carlo simulation (MC) is one of the most used statistical methods that generates a sequence of random numbers. It has been popular in the medical physics because the extent of physical applications that can be simulated and explored by Monte Carlo simulation is wide. The essence of the Monte Carlo simulation is the generation of a random number and repetition of the simulation many times. There are many regular uses for MC, here are some [19]:

- Sampling

  It simply means imitating a real-life system by random generation. A quick example that is also used in this research, light propagation on biological tissues. MC simulates every single photon's random steps through the tissue in the same manner that it behaved in real life.

- Estimation

  Assessment of numerical values related to the used mathematical model for example, the optical properties of a certain object.

- Optimization

  The simplification of complicated systems is a powerful tool that MC uses. Randomness of the applications objects is presented to produce a more efficient way to explore the domain of its function.

3.5.1 Advantages of MC simulation

- *Simplicity*

  MC is easy and flexible. It tends to decrease the complexity level of the model to a group of basic incidents or events. This way makes it possible to translate the behavior of a model in a set of principles.

- *Strength*

  Using randomness as a center of strength is what makes MC so popular over the years. Performing the generation of random numbers and monitoring how the results of the experiments are happening allows to understand the outcomes and also probabilities.

- *Convincing justification*

  The outcomes of the MC simulation are very close to the real model. This semi-accurate resultmakes this simulation reliable and useful in different kind of applications which in turn gives a clear justification of a phenomena.

3.5.2 Monte Carlo simulation of Multi-Layered tissue (MCML)

MCML is one of the most significant simulations ever used especially in the medical applications. It was first introduced by (*Lihong et al,1995*) and until today it's cited as the main research that considers simulating a tissue with multiple layers.

This is a brief explanation of how it works.
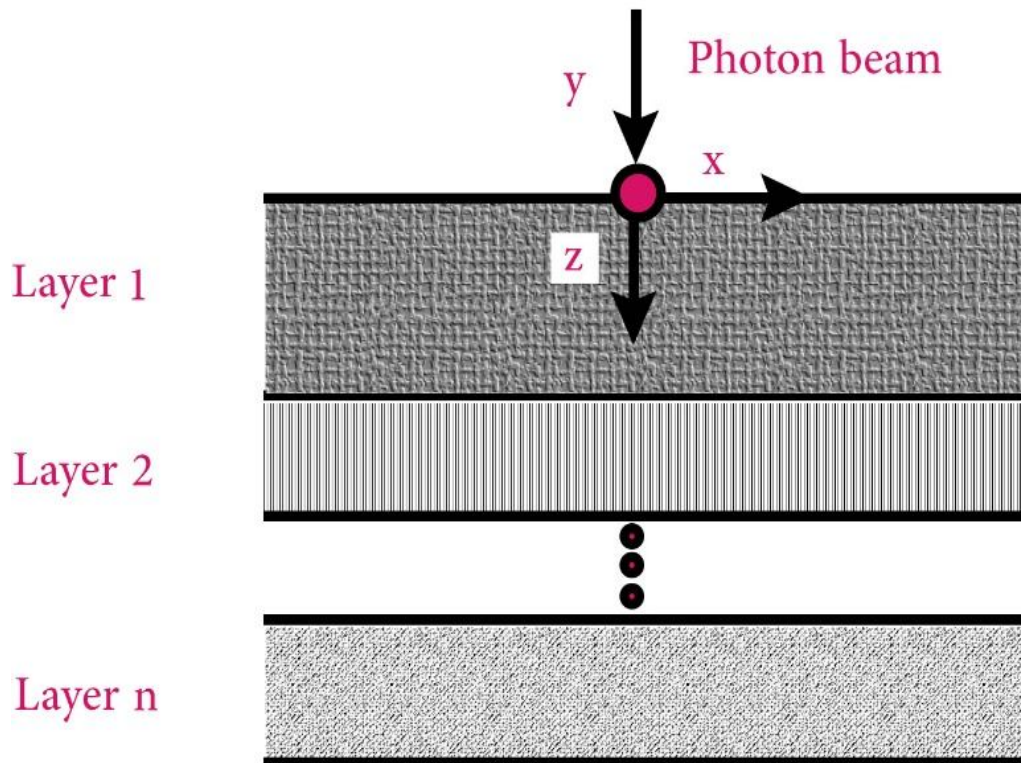
Figure (3.9): A schematic of the Cartesian coordinate system set up on multi-layered tissues. The y-axis points outward.[4]

The main objective of the simulation is to simulate photon's path in turbid medium such as tissues that can be described with their optical properties like absorption and scattering. The model is based on random walk where the photon's steps are traced from where it enters the tissue until it leaves or get fully absorbed. This method follows a set of principles that governs the movement of the photon through the whole process.

Considerations

- The photon propagation principles are expressed as probability distribution for the incremental steps.
- The nature of this method is statistical which requires propagating a large number of photons.
- The number of photons and the computational time are proportional. Every time the number of photons is increased it takes longer time to compute.
- There are three coordinate systems are used in MCML at the same time: The cartesian coordinate system, cylindrical coordinate system and a moving spherical coordinate system.

Assumptions

- Photons are not treated as waves but as neutral particles.
- Multiple scattering of photons by tissues occurs.
  And according to these two assumptions phase and polarization are assumed to be ignored.

MCML steps :

The following algorithm in figure (2.10) explains the MCML steps.
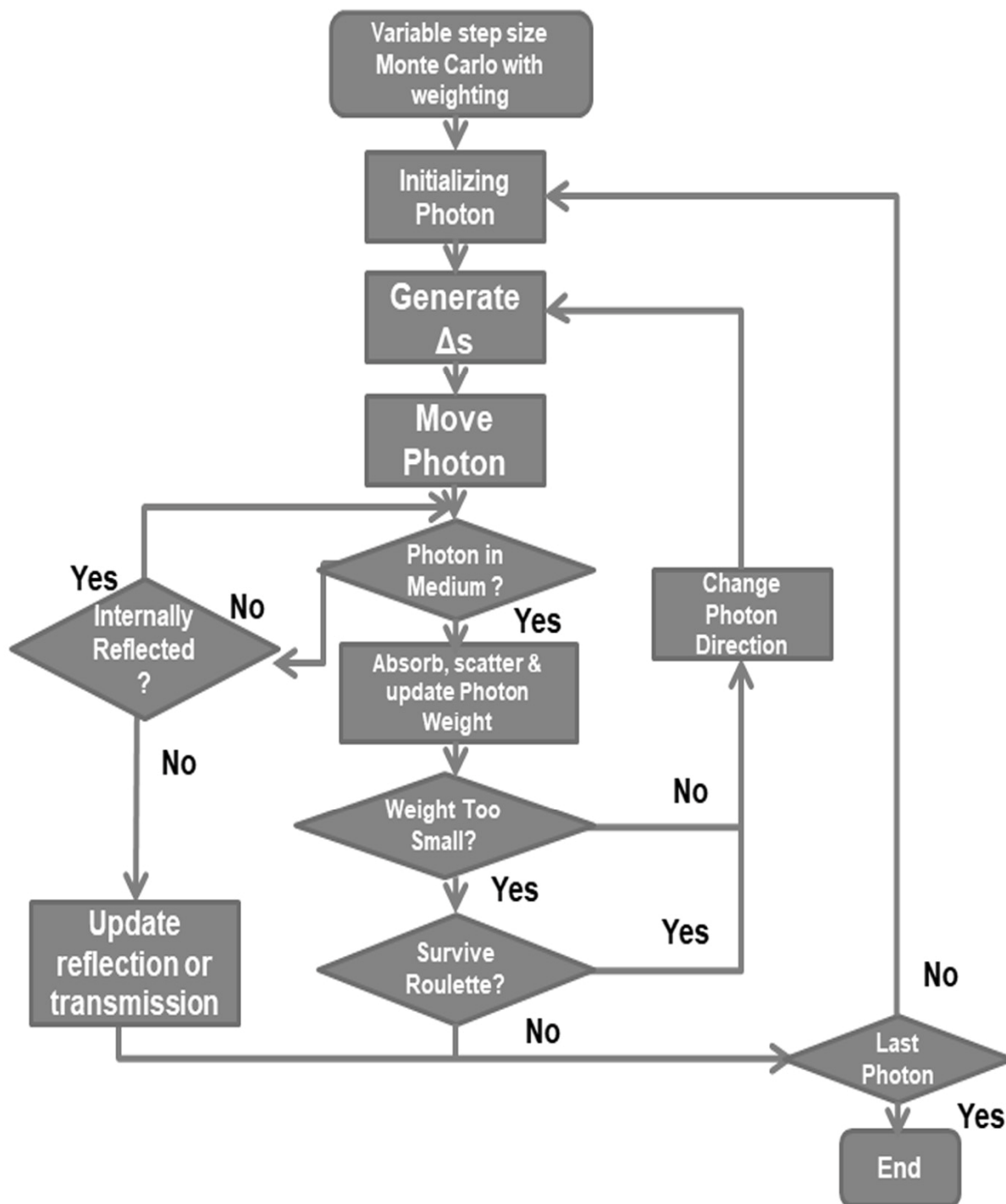
Figure (3.10): MCML algorithm as illustrated by *Lihong, et al*

1) Selecting the variables

The variables that govern the MCML are the step size and the scattering angle (deflection angle θ and azimuthal angle ψ). Figure below was made by candidate.
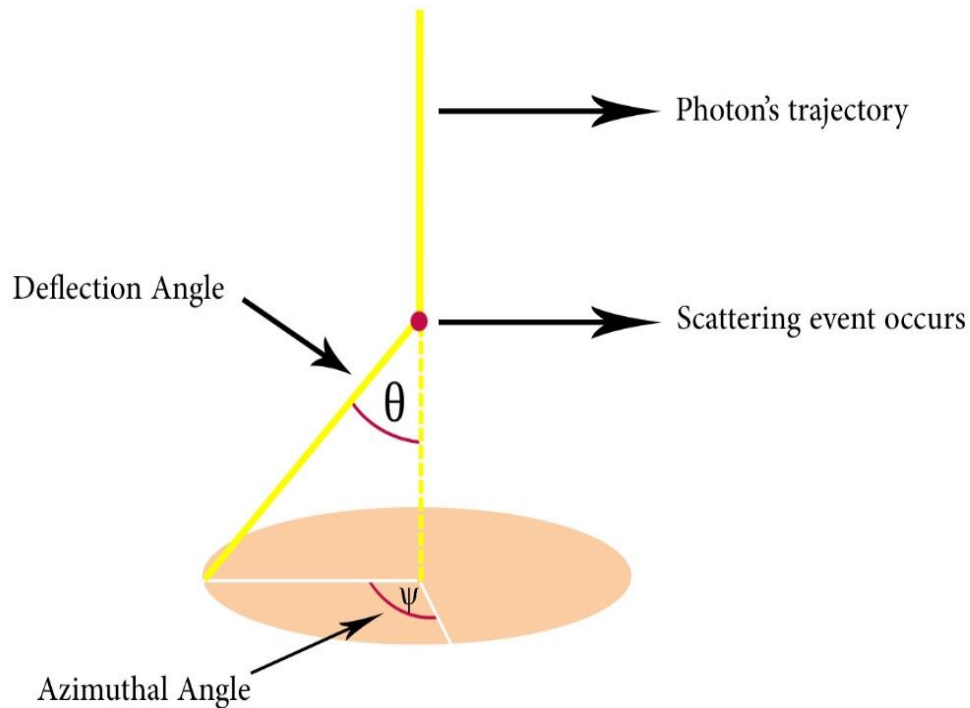
Figure (3.11): Scattering angles

Selection of the step size, deflection angle and azimuthal angle are determined by random number generation. It will be used for sampling from known probability density functions

Sampling random number 'x'

To understand the sampling process at first you need to understand definitions for probability density functions and probability distributions.
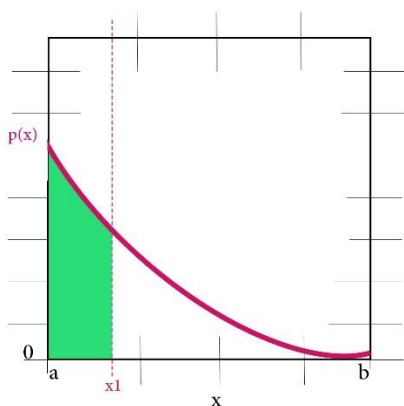
Probability Density Function (PDF) is a function that is defined on a continuous interval describing the area under the curve by unity.

The probability density function p(x) for some random variable, x, defines the distribution of x over the interval a<x<b, such that:

$$\int_{a}^{b} p(x)dx = 1 \qquad (5)$$
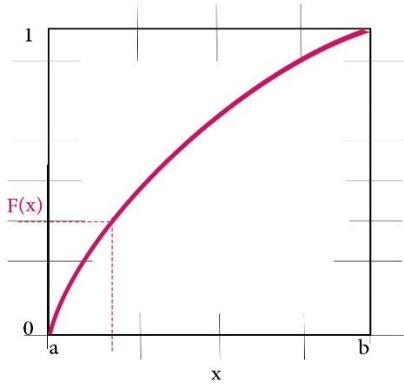
The probability that x will fall in the interval $[a, x_1]$ such that $a < x < x_1$, is given by a probability distribution function, $F(x_1)$ which is defined by:

$$F(x_1) = \int_{a}^{x_1} p(x)dx \qquad (6)$$

A random number generator is used to generate any random number between 0 and 1. By mapping a uniform PDF for the random number (rnd) to a certain PDF p(x) that correspond to step size and the scattering angles.
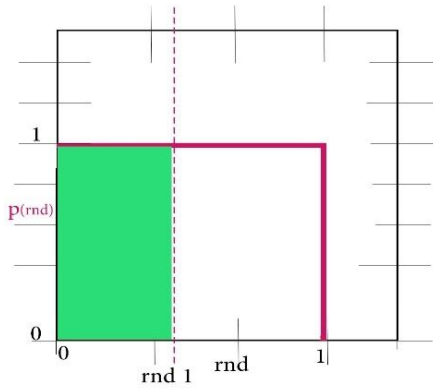
$$\int_{0}^{1} p(rnd)d(rnd) = 1;$$

$$p(rnd) = 1 \, over \, [0,1] \qquad (7)$$

The probability that rnd will fall in the interval $[0, rnd_1]$ such that $0 < rnd < rnd_1$, is given by the probability distribution function, $S(rnd_1)$ which is defined by:
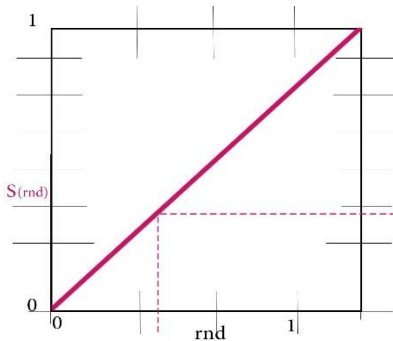
$$S(rnd_1) = \int_{0}^{rnd_1} p(rnd)\,drnd = rnd_1 \qquad (8)$$

$$for \quad 0 \le rnd \le rnd_1$$

The key to the Monte Carlo selection of x using rnd is to equate the probability that rnd is in the interval [0, rnd_1] with the probability that x is in the interval [a,x_1]. By equating the F(x) to S(rnd) and the shaded area ,we get the figure below.
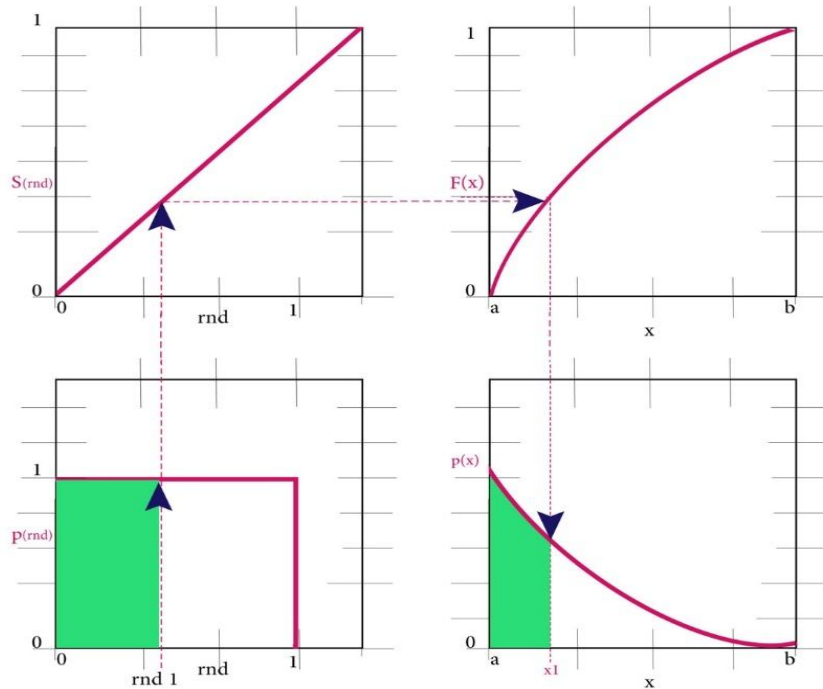
Figure (3.12): Probability Density Function (PDF)[4]

After understanding PDFs and by replacing rnd1 and x1 by the continuous variable rnd and x, the basic equation for sampling x from p(x) using a randomly generated number, rnd over the interval [0,1] :

$$rnd = \int_{a}^{x} p(x)dx$$

(9)

But it's important to note that random numbers need:
- PDFs for step size and the scattering angles and expressing them in terms of rnd.

Step size

$$s = \frac{-\ln(rnd)}{\mu_a + \mu_s} \qquad (10)$$

Deflection angel

$$\theta = \frac{1}{2g}\left[1 + g^2 - \left(\frac{1 - g^2}{1 - g + 2g(rnd)}\right)^2\right] \qquad (11)$$

Azimuthal angle

$$\psi = 2\pi(rnd) \qquad (12)$$

- Relate rnd to PDF using the transformation expression.

2) Initializing photon

Each traced photon is initially assigned a weight, W. This assignment makes it easy to understand the interactions effecting the photon. Before the photon is injected into the tissue at the origin, the weight equals unity.

Specular reflectance is taken into consideration and it happens when there is a mismatched boundary between the outside medium and the tissue. It's expressed by the following equation:

$$R_{sp} = \frac{(n_t - n_m)^2}{(n_t + n_m)^2} \qquad (13)$$

Where R_{sp} is the specular reflectance, n_t is the refractive index of the tissue and n_m is the refractive index of the medium.

Specular reflectance causes a decrease on the photon's weight

$$W = 1 - R_{sp} \tag{14}$$

3) Generating the step size & moving the photon

As explained earlier, the computer's random number generator takes a random variable, rnd, in the interval [0,1] and then samples the step size.

If the photon didn't reach a boundary the position of the photon will be updated by:

$$x \leftarrow x + \mu x.s$$
$$y \leftarrow y + \mu y.s$$
$$z \leftarrow z + \mu z.s \tag{15}$$

4) Update absorption and photon's weight

After the photon takes a step, some of the photon's weight is attenuated due to absorption; the amount of deposited photon weight, ΔQ is:

$$\Delta Q = W \frac{\mu_a}{\mu_a + \mu_s} \tag{16}$$

The new photon weight is updated to:

$$W \frac{\mu_s}{\mu_a + \mu_s} \rightarrow W \tag{17}$$

If scattering occurred, the azimuthal angle $\square$ and the deflection angel θ are taken into account. The final direction of the photon is:

$$\mu_x' = \frac{\sin\theta}{\sqrt{1 - \mu_z^2}} \mu_x \mu_z \cos\psi - \mu_y \sin\psi + \mu_x \cos\theta$$

$$\mu_y' = \frac{\sin\theta}{\sqrt{1 - \mu_z^2}} \mu_y \mu_z \cos\psi - \mu_x \sin\psi + \mu_y \cos\theta$$

$$\mu_z' = -\sin\theta \cos\psi \sqrt{1 - \mu_z^2} + \mu_z \cos\theta \tag{18}$$

If the incident angle is orthogonal to the surface of the tissue the photon direction follows this formula:

$$\mu_x' = \sin\theta\cos\psi$$

$$\mu_y' = \sin\theta\sin\psi$$

$$\mu_z' = SIGN(\mu_z)\cos\theta \tag{19}$$

$$SIGNx = \begin{cases} -1 \text{ if } x < 0 \\ 0 \text{ if } x = 0 \\ 0 \text{ if } x = 0 \end{cases} \tag{20}$$

Then the photon direction is finally updated:

$$\mu_x \leftarrow \mu_x'$$

$$\mu_y \leftarrow \mu_y'$$

$$\mu_z \leftarrow \mu_z' \tag{21}$$

5) Terminating the photon
   The photon is terminated if:
- It escapes the tissue.
- Its weight is decreased inside the tissue below a defined threshold.
   In case the weight decreased inside the tissue, there is a technique called the Russian Roulette used to terminate the photon when

$$W < W_{th} \tag{22}$$

This technique carries out random number generating and offers one last chance in m (e.g., m=10) to survive with a weight of mW. If it doesn't survive it gets terminated.

$$W = \begin{cases} mW \ if & \xi \leq 1/m \\ 0 \ if & \xi > 1/m \end{cases}$$

(23)

6) Internal reflection or escape

By using Fresnel's law, the internal reflectance is calculated.

$$R = \frac{(n_2 - n_1)^2}{(n_1 + n_2)^2}$$

(24)

In case of an escape as an observable reflection, $1 - R(\theta)$ of the current photon weight successfully escapes and updates the total reflectance. But if the photon is internally reflected the new photon weight is updated:

$$W = R(\theta).W$$

(25)

Chapter 4 Methodology

4.1 Model

In this project, two types of models were created, the normal eye model and the diseased eye model. The study is more concerned about the effect of DME on the Outer Nuclear Layer (ONL). In this chapter, the two types of the model are discussed separately according to the selection of optical parameters and layers.

4.1.1 The normal eye model

Circulatory Flat-Top NIR beam

Layer 1 — Cornea

Layer 2 — Aqueous humor, lens and vitreous humor

Layer 3 — Retina, ONL , RPE

Layer 4 — choroid

Light beam

Cornea

Ocular Media

Neural Retina

ONL

RPE

Choroid

Sclera

Figure (4.1): The eye model
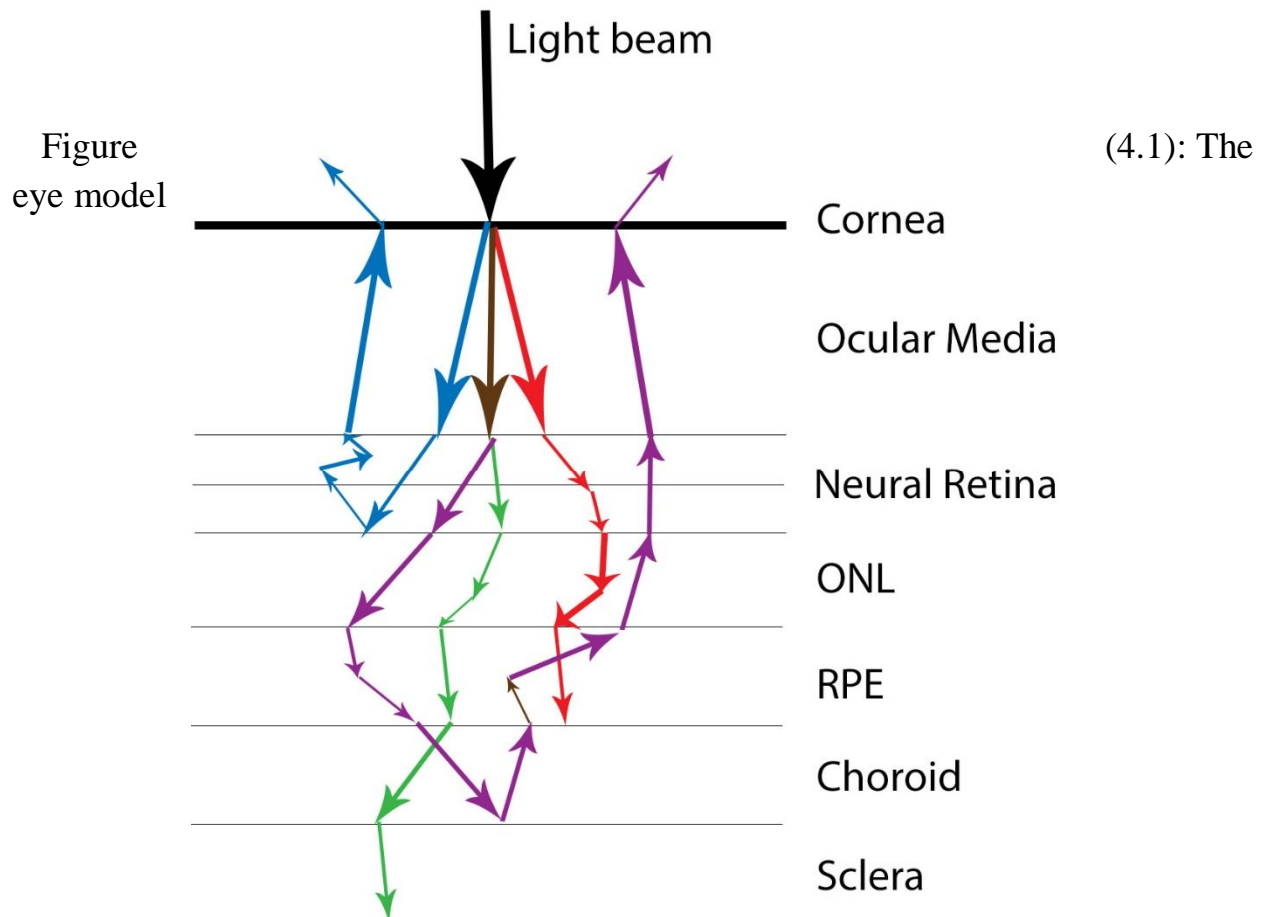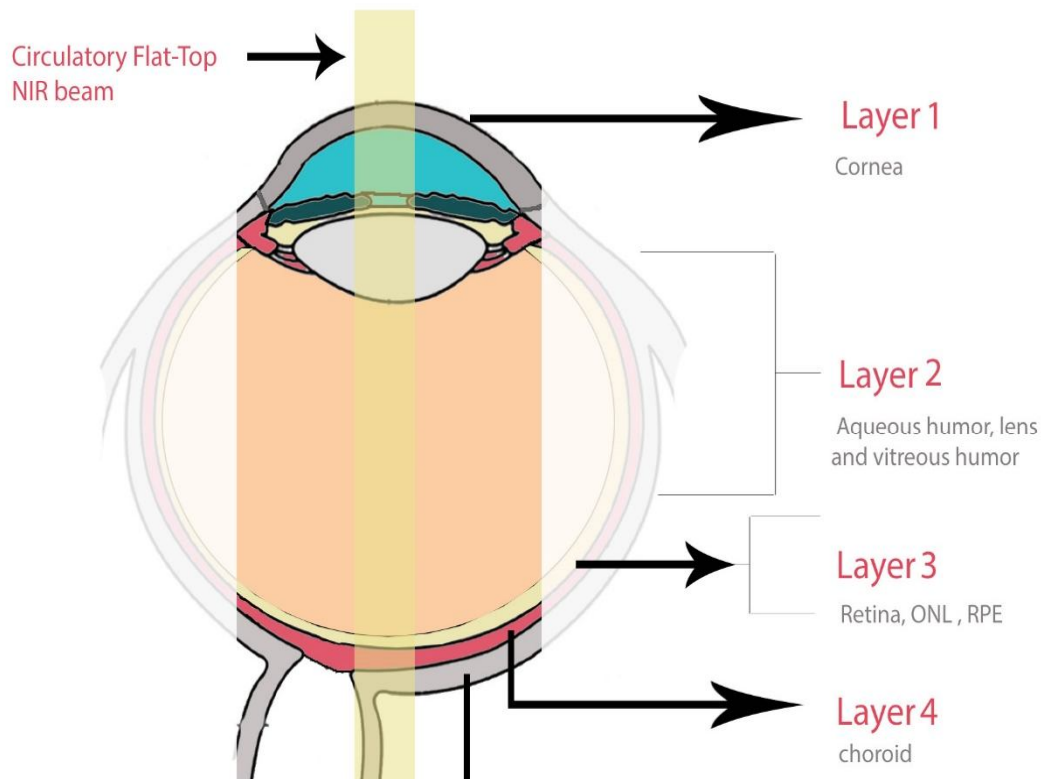
Figure (4.2): Different light interactions on the layers.

As it was discussed earlier, the structure of the eye tissue is the simplest structure in the human body. The light enters the eye starting from the outer coat, the cornea and passes through the eye until it reaches the retina where it's then converted to electrical pulses. The normal eye model expresses the same thing. The normal eye that was modeled is amodified Styles et al [20]model. Alterations in the model was adding the ONL layer between the retina and the RPE, modelling the cornea layer and changing the transmission values of the ocular media. Each layer is described by its optical parameters. Figures above were made by candidates.

As there is no available study including all the estimations of the optical properties of the eye. The values used were chosen according to several studies and assumptions.

Assumptions and calculations

As there were no direct data considering the absorption and scattering coefficients available and there were no known direct formulas for both coefficients, calculations were made by derivation from different mathematical terms.The ocular media& cornea transmission spectra obtained from [9] respectively, is illustrated in the figures below.
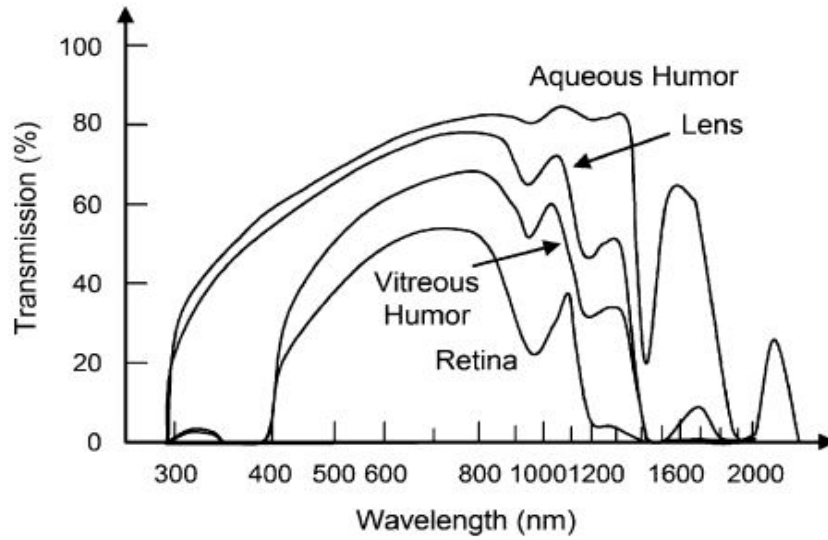
Figure (4.3): Ocular media and retina Transmission spectrum. All transmission losses are accounted for, including those due to absorption and scattering.[9]
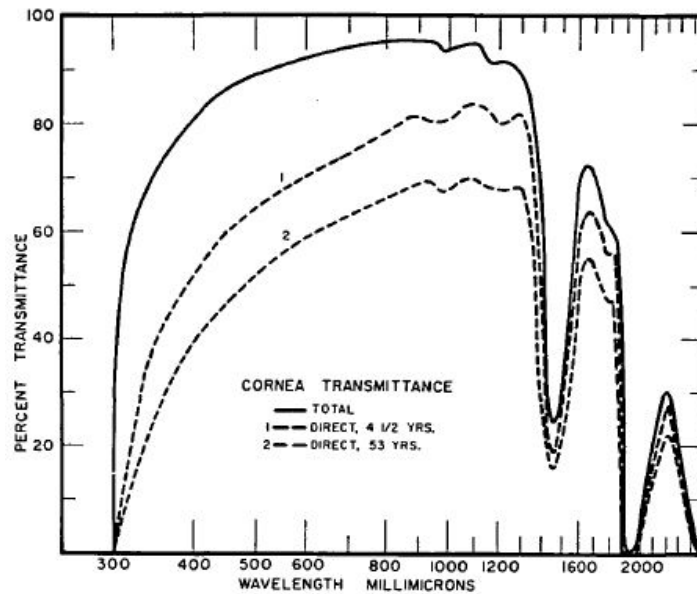
Figure (4.4): Transmission of cornea. [21]

From the spectra, transmission values were taken at 870 nm. The table below shows the data that was obtained from the plot.

Table (4.1): Transmission values of ocular media and Neural retina

Layer	Transmission (T%)

Cornea	95 %
Aqueous humor	81 %
Lens	75 %
Vitreous humor	63 %
Neural Retina	39 %

Transmission is related to absorbance by the equation:

$$A(absorbance) = 2 - \log_{10} \%T \qquad (26)$$

And absorbance is related to absorption coefficient by the formula:

$$\mu_a = \frac{2.303A}{t} \qquad (27)$$

The scattering coefficient value calculation needs a little explanation.

In chapter 3.4.2, a brief definition of optical depth describes that it has a relationship with transmission and according to the following equation, the optical depth can be expressed by:

$$T = e^{-\tau}$$

(28)

Taking natural logarithm for both sides, we get:

$$-\ln(T) = \tau$$

(29)

By substituting the values with the values obtained from the transmission plot in table (4.1.12), optical depth was calculated.

The optical depth has a relationship with the scattering coefficient too, explained in the formula:

$$\tau = t(\mu_s + \mu_a) \qquad (30)$$

By substituting the values that was calculated in the previous equations, the scattering coefficient (μ_s) can be obtained.

The anisotropy factor was assumed according to [5], where the optical properties with three wavelengths were obtained 980, 1310 and 1530. Assumption was based on increase and decrease of the value.

Table (5.1) shows the optical properties of the normal eye that were used with a Near-Infrared wavelength selection of 870.

4.1.2 The diseased eye model.

The ONL layer was chosen to be the layer to be studied. The layer that holds the rods and cones cell body presents the characteristics of DME. Correia et al [3] modeled this layer with increased ONL thickness and obtained the optical properties that is used also in this research model. By keeping the other layers with the same properties, the ONL parameters are changed.

4.2 MCML software

Lihong et al [4] created an available software for public domain follows the same method that was explain on chapter 3.

http://omlc.org/software/mc/mcml/index.html
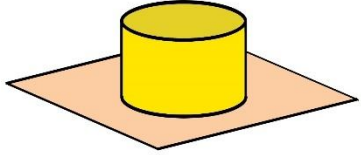
The input file of both eye models can be found in Appendix I.

The output files were later in turn read by a MATLAB program lookmcml.m and subroutine getmcml.m that reads the output file and generates a colormap using makec2f.m. The MATLAB codes are provided on the website above too.

Beside the model optical properties, there are other requirement for the output data

Table (4.2): Additional MCML software requirements.

Input	Value	Comment
Number of photons	1000000 photons	-
Energy(J)	2.28326182E-19 J	$E = \dfrac{hc}{\lambda}$
		Separation between 2D-

Grid separations (Δr&Δz)	Δr 0.010 Δz 0.010	homogeneous grid lines in z and r direction for photon absorption. It should be large enough to give an acceptable variance and small enough to give an acceptable resolution.
Number of grid elements Nz, Nr and Nα, respectively.	250 250 1	Alpha is the angel spanned between the photon exiting direct on and the surface normal. Δα(separation)=0 and There was no need to resolve one of the directions (z, r or α) so Nα=1.
Beam specification	Flat-top circulatory beam	 Flat-top circular beam
Refractive index for the top ambient medium above the first layer	1.0	Refractive index of air
Refractive index for the bottom ambient medium below the last layer	1.0	Refractive index of air

Chapter 5 Results and discussion

Table (5.1) and table (5.2) represent the model of the normal eye and the diseased eye respectively as they were described by their parameters.

The blue shading in table (5.1) represent information obtained from variety of studies while the red shading is based on assumptions and calculations that were explained in chapter 4. An important note to mention is that two layers of the neural retinal layer were used as layer 7 and 8 to make an interface between the neural retinal layer and photoreceptors within it by inserting a layer simulating that interface. The diseased eye model only differs on the ONL layer

Table (5.1): Optical properties of healthy eyes used in Monte Carlo Simulation.µa=absorption coefficient, µs=scattering coefficient, d=thickness, g=anisotropy factor, n=refractive index.

Layer number	Layer	µa (cm-1)	µs (cm-1)	d (cm)	g	n	References
1	Cornea	0.097	0.001	0.52	0.7	1.38	[21] [9]
2	Aqueous Humor	0.69	0.01	0.3	0.8	1.33	[9] [5]
3	Lens	0.86	0.047	0.32	0.8	1.39	[9] [5]
4	Vitreous Humor	0.31	0.002	1.5	0.8	1.33	[9] [5]
5& 6	Neural Retina	42.9	0.09	0.022	0.97	1.33	[9]
7	ONL	5.4E-10	1.28E-5	0.007	0.995	1.39	[3]
8	RPE	3.336	0.016	0.001	0.84	1.4	[22]
9	Choroid	0.535	5.206	0.01	0.89	1.35	[22]
10	Sclera	0.003	5.484	0.07	0.9	1.3	[22]

Table (5.2): ONL layer with visible thickness due to DME.[3]

Layer	µa(cm-1)	µs(cm-1)	d(cm)	g	n
ONL	5.4E-10	7.7E-6	0.012	0.995	1.39

As one can see clearly, the differences are mainly presented in the increase of the thickness and the decrease of scattering coefficient.

A colormap plot in figure (5.2) and figure (5.3) shows the energy deposition $A(z,r)$ and photon fluence $F(z,r)$ in the grid system. $A(z,r)$ gives the absorbed photon probability density in cm-3 and by dividing it by the absorption coefficient cm-1 it can be converted to $F(z,r)$ cm-2. The light is delivered as a point source of collimated light at r = 0, z = 0. The colorbar is a logscale. Note how $A(z,r)$ is discontinuous at the boundaries between layers with different absorption coefficients.

Comparing the results obtained from the colormap plot, it can be seen that a scattering event decreased at nearly the end of the light path in the DME plot where the ONL layer is presumed to be there.

As a justification for the results, what really happens when a diabetic macular edema occurs is as it was explained earlier on chapter 3, the BRB breakdown results in leaking fluid inside the tissue leading to swelling which effected the thickness of the layer as it increased to nearly twice. The main type fluids that leak are Hemoglobin, water and lipid. These types of fluids are also considered the main NIR light absorbers and by that it reduces the scattering event as it can be seen in table (5.2) the scattering event decreased to approximately one and three-fifth. By the time this amount of fluid grows as a consequence of late treatment, it prevents light from passing through to the retina which may lead to partial vision loss or visual impairment in late cases.

Another justification considered by *Correia,et al* is as we quote :

"The increase in thickness leads to a reduced backscattered signal compared to the healthy status. This is in agreement with the theory, as the same number of nuclei within a larger volume should produce less backscattering." [3]

ONL layer holds the cell bodies of rods and cons, so the increase in their thickness produce less backscattering.

Figure (5.1): Colormap of the Monte Carlo Normal eye output from MCML.
(TOP) The energy deposition A(z,r) [J/cm3 per J delivered].
(BOTTOM) The fluence rate F(z,r) [J/cm2 per J delivered].
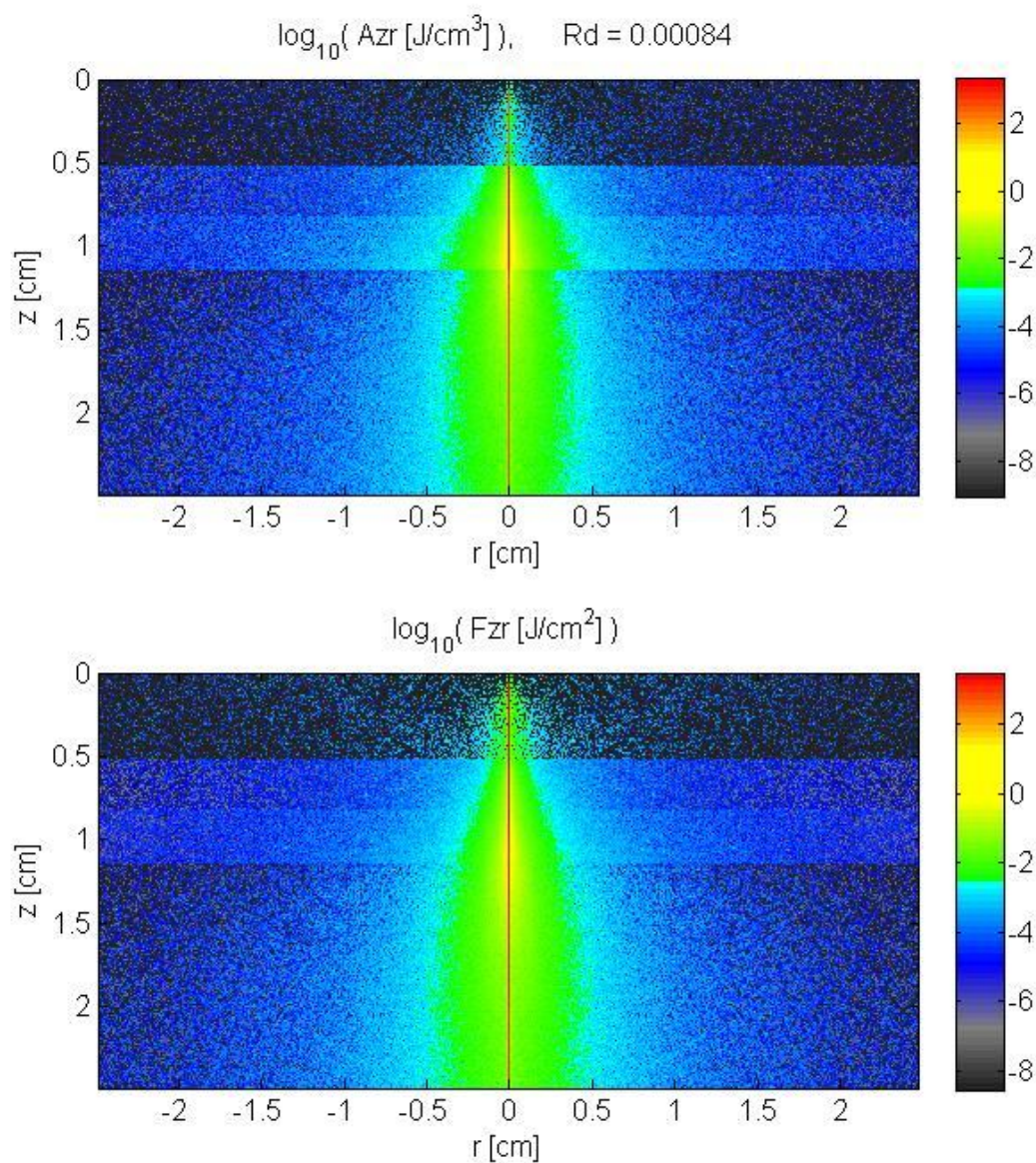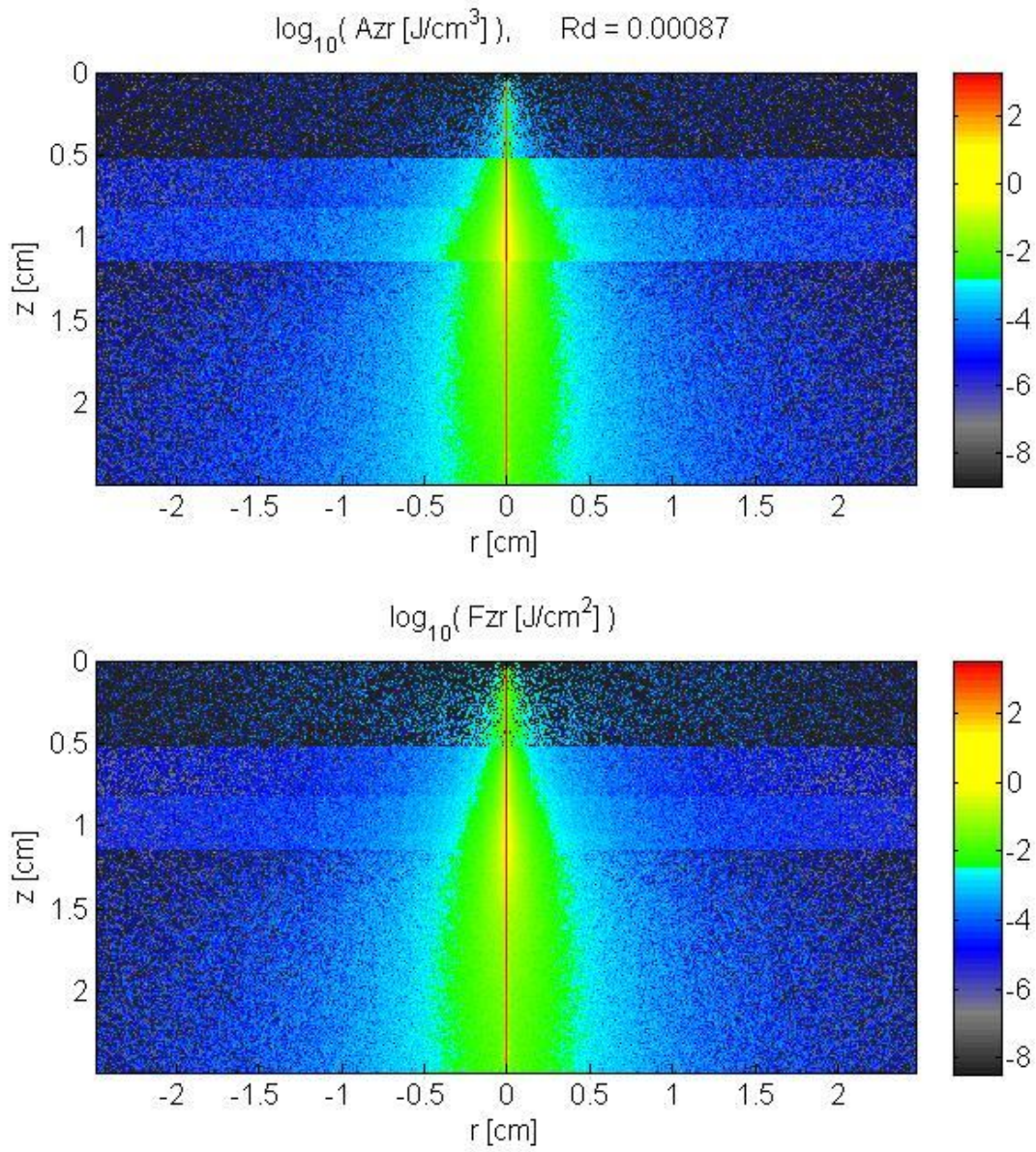
Figure (5.2): Colormap of the Monte Carlo DME eye output from MCML.
(TOP) The energy deposition A(z,r) [J/cm3 per J delivered].
(BOTTOM) The fluence rate F(z,r) [J/cm2 per J delivered].

Chapter 6 Conclusion and recommendations

The project was completed according to suggested plan; After the data was collected from various references, calculations were obtainedby derivation from different mathematical terms and appropriate assumptions were considered, the output files of the models' parameters were simulated using a suitable software providing the desired results where comparison between the two models were made. MCML represented an important method in simulating tissues models with multiple layers as it considers the light entering the tissue as a packet of photons, each individual photon's random walk is traced as it interacts with the tissue. The simplicity and flexibility of this type of Monte Carlo method made it suitable for these kinds of projects. The results displayed the differences between the healthy and the diseased cases where a comparison showed a decrease in the scattering event justified due to the main absorbers of the NIR light that leaks into the eye from the BRB (water, hemoglobin, lipid) and if they continue to leak without treatment this may lead to vision loss in late cases. Another justification is that the increase in thickness of the cell bodies of ONL that leads to reduce the backscattering light. Another effect caused by the disease is the increase in thickness due to the swelling of the layer obviously because of the fluid leak.

However, we aim to extend the project to simulate the whole retina instead of the three layers that were used and we recommend to continue exploring the other retinal layers effected by DME and also building models for other eye diseases to enrich the information of such cases.

References

[1] S. R. a. T. W. G. Cohen, "Diabetic Retinopathy and Diabetic Macular Edema," *Dev Ophthalmol,* vol. 55, pp. 137-146, 2016.

[2] E. S. e. a. Elwali, "Frequency of diabetic retinopathy and associated risk factors in Khartoum, Sudan: population based study," *Int J Ophthalmol,* vol. 10, no. 6, pp. 948-954, 2017.

[3] L. P. A. A. S. B. F. C. P. M. Ant´onio Correia, "Monte Carlo Simulation of Diabetic Macular Edema Changes on Optical Coherence Tomography Data," in *Biomedical and Health Informatics (BHI), 2014 IEEE-EMBS International Conference on*, Valencia, Spain, 2014.

[4] S. L. J. a. L. Q. Z. L. H. Wang, "tissues, MCML - Monte Carlo modeling of photon transport in multi-layered," *Computer Methods and Programs in Biomedicine,* vol. vol. 47, p. pp. 131–146, 1995.

[5] D. K. e. a. Sardar, "Optical properties of ocular tissues in the near infrared region," *Lasers Med Sci,* vol. 22, no. 1, pp. 46-52, 2007.

[6] J. Cunha-Vaz, "The Blood-Retinal Barrier in the Management of Retinal Disease: EURETINA Award Lecture," *Ophthalmologica,* vol. 237, no. 1, pp. 1-10, 2017.

[7] M. e. a. Santos, "Simulation of cellular changes on Optical Coherence Tomography of human retina," *Conf Proc IEEE Eng Med Biol Soc,* vol. 2015, pp. 8147-50, 2015.

[8] B. R. a. R. C. Mackenna, Illustrated physiology, Edinburgh: Churchill Livingstone, 1997.

[9] I. P. Herman, Physics of the Human Body, Springer, 2007.

[10] 2. a. t. W. M. The Vitreous Humor Archived April 26, "Wayback machine," [Online].Available: https://web.archive.org/web/20070426073939/http://retina.anatomy.upenn.edu/~lance/eye/humor_vitreous.html.

[11] Wei Gao, Erika Tátrai, Veronika Ölvedy, Boglárka Varga, Lenke Laurik, Anikó Somogyi, Gábor Márk Somfai, Delia Cabrera DeBuc, "Investigation of changes in thickness and reflectivity from layered retinal structures of healthy and diabetic eyes with optical coherence tomography," *Journal of Biomedical Science and Engineering,* vol. 4, pp. 657-665, 2011.

[12] O. M. F. Lee Ann Remington, Clinical antomy and physiology of the visuaal system, St. Louis, Missouri: Elsevier, 2012, p. 71.

[13] G. e. a. Virgili, "Optical coherence tomography versus stereoscopic fundus photography or biomicroscopy for diagnosing diabetic macular edema: a systematic review," *Invest Ophthalmol Vis Sci,* vol. 48, no. 11, pp. 4963-73, 2007.

[14] C. D. Y. T. a. P. X. Ning Liu, "Virtual-OCT: A simulated optical coherence tomography instrument," *Journal of Innovative Optical Health Sciences,* vol. 7, no. 5, p. 12 , 2014.

[15] J. G. e. a. Fujimoto, "Optical biopsy and imaging using optical coherence tomography," *Nat Med,* vol. 1, no. 9, pp. 970-2, 1995.

[16] I. P. J. C.-V. C. Lobo, Diabetic macular edema, Springer, 2012, pp. 1-21.

[17] J. Byrnes, Unexploded Ordnance Detection and Mitigation, Springer, 2009, pp. 21-22.

[18] e. a. M. HeiliRo, Mathematical Modelling, Switzerland: Springer, 2016.

[19] D. B. T. T. a. B. Z. Kroese, "Why the Monte Carlo method is so important today ?," *Wiley Interdisciplinary Reviews: Computational Statistics,* vol. 6, pp. 386-392, 2014.

[20] I. B. e. a. Styles, "Quantitative analysis of multi-spectral fundus images," *Med Image Anal,* vol. 10, no. 4, pp. 578-97, 2006.

[21] E. A. & W. J. R. Boettner, "Transmission of the ocular media," *Investigative ophthalmology & visual science,* vol. 6, no. 1, pp. 776-783, 1962.

[22] M. e. a. Hammer, "Optical properties of ocular fundus tissues--an in vitro study using the double-integrating-sphere technique and inverse Monte Carlo simulation," *Phys Med Biol,* vol. 40, no. 6, pp. 963-78, 1995.

Appendix

```
1.0                                          # file version
2                                            # number of runs


### Specify data for run 1
Normal2.mco      A                           # output filename, ASCII/Binary
1000000                                      # No. of photons
0.01      0.01                               # dz, dr
250       250      1                         # No. of dz, dr & da.

10                                           # No. of layers
# n       mua      mus      g        d       # One line for each layer
1.0                                          # n for medium above. Air
1.38      0.097    0.001    0.7      0.52     # layer 1 Cornea
1.33      0.69     0.01     0.8      0.3      # layer 2 Aqueous
1.39      0.86     0.047    0.8      0.32     # layer 3 Lens
1.33      0.31     0.002    0.8      1.5      # layer 4 Vitreous
1.33      42.9     0.09     0.97     0.022    # layer 5 Neural Retina
1.33      42.9     0.09     0.97     0.022    # layer 6 Neural Retina 2
1.39      5.4E-10  1.28E-5  0.995    0.007    # layer 7 ONL
1.4       3.34     0.016    0.84     0.001    # layer 8 RPE
1.35      0.54     5.206    0.89     0.01     # layer 9 Choroid
1.3       0.003    5.484    0.9      0.07     # layer 10 Sclera
1.0                                          # n for medium below. Air
```

```
1.0                                          # file version
2                                            # number of runs


### Specify data for run 1
DME2.mco         A                           # output filename, ASCII/Binary
1000000                                      # No. of photons
0.01      0.01                               # dz, dr
250       250      1                         # No. of dz, dr & da.

10                                           # No. of layers
# n       mua      mus      g        d       # One line for each layer
1.0                                          # n for medium above. Air
1.38      0.097    0.001    0.7      0.52     # layer 1 Cornea
1.33      0.69     0.01     0.8      0.3      # layer 2 Aqueous
1.39      0.86     0.047    0.8      0.32     # layer 3 Lens
1.33      0.31     0.002    0.8      1.5      # layer 4 Vitreous
1.33      42.9     0.09     0.97     0.022    # layer 5 Neural Retina
1.33      42.9     0.09     0.97     0.022    # layer 6 Neural Retina 2
1.39      5.4E-10  7.7E-6   0.995    0.012    # layer 7 ONL(DME)
1.4       3.34     0.016    0.84     0.001    # layer 8 RPE
1.35      0.54     5.206    0.89     0.01     # layer 9 Choroid
1.3       0.003    5.484    0.9      0.07     # layer 10 Sclera
1.0                                          # n for medium below. Air
```